The 6th International Conference on Applied Energy – ICAE2014

Preparation and Characterization of hyperbranched oligomer modified LiMn2O4 thin film cathodes

Cheng-Lun Chen [a,b,]*, Kuo-Feng Chiu [a], Hoang-Jyh Leu [b], Chen Chung Chen [c], Chang-Rung. Yang [c]

[a] Department of Materials Science and Engineering, Feng Chia University, 40724, Taichung, Taiwan
[b] Department of Fiber and Composite Materials, Feng Chia University, 40724, Taichung,Taiwan
[c] Materials Research Laboratories, Industrial Technology Research Institute, 310, Hsinchu, Taiwan

Abstract

The LiMn2O4 thin film electrode modified by hyperbranched oligomer has been prepared and studied. The hyperbranched oligomer can be self-polymerized for reducing the thermal-runaway hazard by the internal short protection mechanism in lithium ion batteries. The influence of the oligomer coating on cathode has been studied with the binder/carbon-free thin film. In the various C-rate charged-discharged tests, there are no significant differences between the cells with/without the oligomer coating. In this research, the hyperbranched oligomer additive acts as a protection to improve the thermal stability of LiMn2O4. Therefore, the property of thermal stability and its function in safety may benefit the future development of electric vehicles.

1. Introduction

Lithium ion batteries have been the most popular energy devices for mobile devices (e.g., mobile phone, touch panel and notebook); and further, the energy devices have been designed and applied to electric vehicles (EVs) and hybrid electric vehicles (HEVs). [1-4] According to the different purposes, lithium ion batteries were usually studied and improved for the power density, energy density and cycle life. However, a high energy density device with humans should be considered and designed for safety precaution. In order to improve the stability and safety of lithium ion battery, some materials of the component parts have been studied to modify and substituted. For example, the commercial cathode LiCoO2 has been replaced with LiMn2O4 and LiFePO4 gradually, due to its toxicity, high cost, and instability at high voltages [5-7]. Moreover, inorganic electrolyte and electrolyte additive has been developed in industry application, such as polymer electrolyte and vinylene carbonate additive [8-12]. To

* Corresponding authors: Tel:+ 886-4-24517250 Ext. 5342 ; Fax: +886-4-24510014;
Email: jack231010@yahoo.com.tw

consider for safety, polyethylene (PE), polypropylene (PP) and PP/PE composite separators are usually utilized to separate electrodes to prevent the internal short circuit. Due to the melting points of these polymers are as low as 110-140 ^{o}C, searching a material for the second protection is necessary. Wang et al. have studied a self-polymerized membrane derivative of a branched additive to reduce the danger of lithium ion batteries [13]. The self-polymerized mechanism was as an internal short protection, which work around 200-230 ^{o}C and prevent the thermal run away of batteries [14-17]. In these simulating internal short examinations, the safety mechanism of oligomer additive have been tested and proven by the nail penetration tests [13, 17].

In our previous research [18-20], $LiMn_2O_4$ thin film has been deposited and studied for the electrochemical performance of cathode in lithium battery. The $LiMn_2O_4$ thin film electrode exhibits a stable cyclability and a specific capacity (~ 110 mAh/g under room temperature), which are greatly applicable to study the simple characteristics of pure cathode active material. The present study of the hyperbranched oligomer additive is based on the researches of Industrial Technology Research Institute (ITRI) in Taiwan [13-17]. And, the hyperbranched oligomer has been coated on pure $LiMn_2O_4$ thin films to form the composite electrodes without the influence of binder and conductive carbon. The electrochemical performances of the composite electrodes have been studied, in which the charged-discharged tests and the electrochemical impedance spectra have revealed the effects of the hyperbranched oligomer on pure $LiMn_2O_4$ thin film cathode.

2. Experimental

The $LiMn_2O_4$ thin films (labelled as LMO) were deposited on stainless steels and silicon discs by radio frequency sputter method detailed in our previous study [18-20]. The thin films were annealed at a temperature of 600 ^{o}C for 1 hour in air. In ITRI, the as-prepared oligomer solution was synthesized with BMI and BTA in n-methyl-2-pyrrolidone (NMP). The solution was coated on LMO electrode to form the hyperbranched oligomer/$LiMn_2O_4$ composite electrode (labelled as B-LMO) and dried at 60 ^{o}C for 6 hour. The thermogravimetric analysis (TGA) and differential scanning calorimetric analysis (DSC) of the dry oligomer powder were carried out on a SDT2960 thermal analyzer (TA Instrument, U.S.A.), at a heating rate of 10 ^{o}C/min. The surface morphologies of the thin film electrodes were observed by a field-emission scanning electron microscope (FE-SEM, JEOL JSM-6700) at an accelerating voltage of 3 kV and a current of 10 mA. The X-ray photoelectron spectroscope (XPS, ULVAC-PHI) was used to detect the composition on surface and inside of the thin films. In an Ar filled glove box, the LMO and B-LMO electrodes were packed in conventional coin cells (2032 type) with lithium foils as the counter and reference electrodes. The electrolyte was 1 M $LiPF_6$/ethyl carbonate/ethyl methyl carbonate (volume ratio of 1:2) solution. The charged-discharged tests were carried out by using an electrochemical measurement system (Jiehan 5600 from Jiehan Technology, Taiwan). The cells were charged to 4.3 V and discharged to 3.0 V under a constant current. The current density range was operated in 0.024-1.2 A/g, i.e. 0.2 C to 10 C for battery. The electrochemical impedance spectra (EIS) were measured on a Hioki 3522-50 analyzer over the frequency range of 10^5-10^{-2} Hz.

3. Results and discussion

3.1. TGA and DSC

The DSC and TGA plots of hyperbranched oligomer (after drying at 60 ^{o}C) are presented in Fig. 1. In DSC and TGA plots, the reaction peaks observed around 80-135 ^{o}C are due to the combination of adsorbed water evaporation and residual solvent, where the related content is about 10 wt%. A broad peak

is detected around 200 ^{o}C, which is attributed to that hyperbranched oligomer is cross-linked drastically to polymerize as a hyperbranched polymer products. The hyperbranched polymer products can suppress the thermal runaway induced by internal short event in lithium battery system [13, 14, 17].
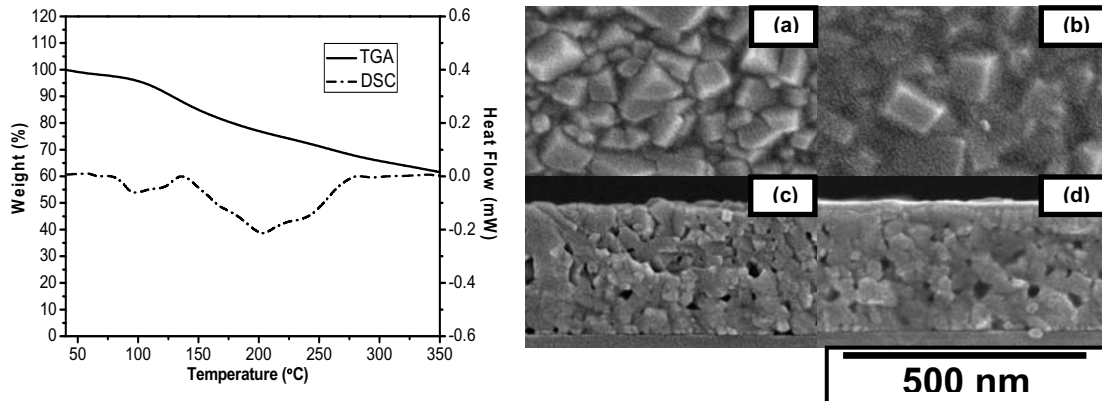

Fig. 1 TGA (solid line) and DSC (dash line) plots of the hyperbranched oligomer. The weight of the detected sample is 2.28 mg.
Fig. 2 SEM plane view images of (a) LMO, (b) B-LMO thin films, and the cross-section image of (c) LMO, (d) B-LMO thin films.

3.2. SEM morphology

As shown in Fig. 2a, the top view image show a clear surface morphology of the LMO thin films. The morphology is composed of the $LiMn_2O_4$ grains (~150 nm) exhibited sharp facets. In contrast to LMO, the surface morphology of B-LMO is slightly indistinct and exhibits some electron damage, in which it has been proven that the hyperbranched oligomer have been coated on the $LiMn_2O_4$ thin film (shown in Fig. 2b). According to the cross section image (Fig. 2c and Fig. 2d), it has been found that the oligomer layer is smooth and contacts well with the $LiMn_2O_4$ film. The thickness of $LiMn_2O_4$ and the oligomer thin film are 430 nm and 25 nm.

3.3. XPS analyse

Fig. 3 shows the XPS spectra of B-LMO, where the solid line and the dash line represent the inside and the surface of B-LMO thin film, respectively. The peak at the binding energy of 400.0 eV represents $-$C$-$N$-$ bonding due to maleimide groups of the BMI/BTA-based oligomer in the N1s spectra, as shown in Fig. 3. The peak intensity of the film on surface is more higher than the inside in N1s spectra, because most of the oligomer have been removed on B-LMO sample after Ar ion etching (the 3 min etching for deep-profile composition analysis). According to the N1s data, it has been proven that the hyperbranched oligomer layer exists on the surface of $LiMn_2O_4$ film and the thickness may be thinner, which is consistent with the SEM result.
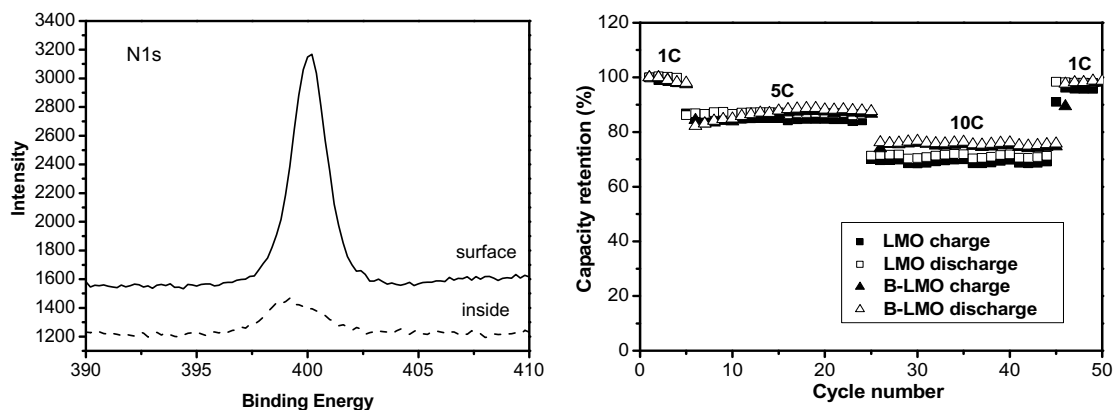
Fig. 3 XPS spectra of N1s for (solid line) surface analyses and (dash line) inside of B-LMO thin film.
Fig. 4 Charged-discharged performance of the LMO and B-LMO thin film electrodes cycled at 1 C, 5 C and 10 C, in the range of 4.3 V to 3.0 V (vs. Li/Li$^+$).

3.4. Charged-discharged test

Therefore, the B-LMO electrodes with thinner oligomer layer have been tested for cycle life and charged-discharged at the high rates (1 C, 5 C, and 10 C), as shown in Fig. 4. At the discharged rates of 5 C and 10 C, the capacity retentions of the B-LMO electrode are comparable to the LMO electrode. And, the both electrodes show excellently fast charge-discharge cyclability (~98 % retention) after 50 cycles with various rates (1 C~10 C). The result indicates that there is no significant influence in capacity while the B-LMO electrodes are operated at the fast charged-discharged rates.

3.5. Electrochemical impedance spectra

For the purpose of studying the effect of the hyperbranched oligomer coating upon the $LiMn_2O_4$ electrodes, the EISs have been used to analyze the interfacial resistances of LMO and B-LMO electrodes before and after cycling, as shown in Fig. 5. All of the EISs consist of semicircles at high frequency and an inclined line at low frequency. And, the curves can be well fitted by a equivalent circuit (insert in Fig. 5a), where Re denotes the electrolyte resistance; Rsei and CPE1 represent the resistance and the constant phase element for the interface of the solid electrolyte interphase (SEI)/$LiMn_2O_4$; Rct and CPE2 represent the charge transfer resistance and the electric double layer; the Warburg element (W) represents the semi-infinite diffusion in the $LiMn_2O_4$ electrode. Before cycling (Fig. 5a), the EIS of B-LMO electrode shows an observably larger internal resistance with a wider semicircle than the LMO electrode. It is attributed to the initial oligomer coating on the electrode surface, which can be seen as a resistor, Rsei (98.6 Ω). After charge-discharge cycling (Fig. 5b), the EIS of B-LMO shows a significant reduction of the semicircle in comparison with the B-LMO electrode without cycling, and the Rsei is decreased to 48.4 Ω. It may be attributed to the formation of the oxidative SEI derivative based on maleimide, which is induced by the self-polymerization of the hyperbranched oligomer after charged process [13]. This SEI derivative may be composed of the electrolyte and the higher molecular weight hyperbranched oligomer. The data of the EISs indicate that the oxidative SEI derivative exhibits a lower resistance, and it may not cause a significant effect for the lithium ions migrating.
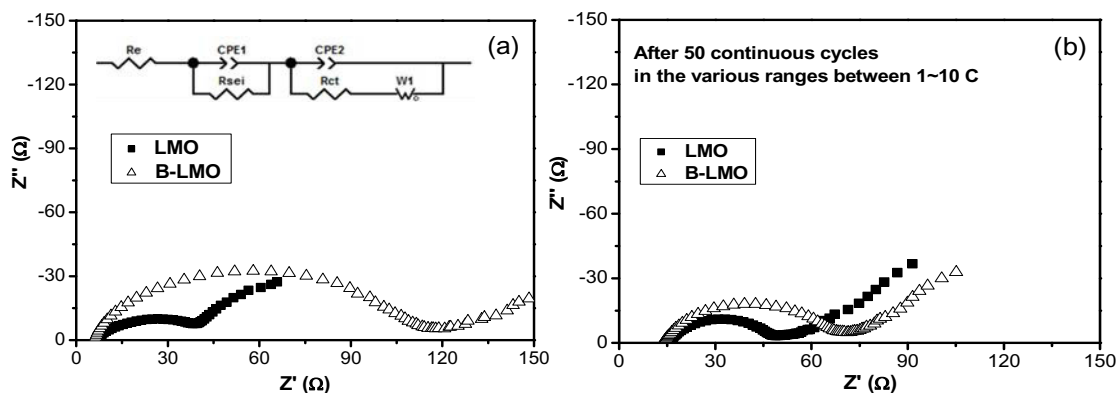
Fig. 5 The EISs of electrodes before and after 50 cycles. (a) before cycling (b) after cycling. The insert is the equivalent circuit in Fig. 5 (a).

4. Conclusions

The researches have confirmed that the BMI/BTA-based oligomer functioned not only as a protection of internal short circuit, which also exhibits positive effects for $LiMn_2O_4$ electrode, at an elevated temperature especially. At a room temperature, there is no significant influence in the high rate charge-discharge tests for the electrode with the oligomer coating. The electrochemical characteristic is attributed to the oligomer coating and its self-polymerization mechanism. After a charge process, the oligomer coating is synthesized to an oxidative SEI derivative, which can reduce the capacity fading of the $LiMn_2O_4$ electrode due to the operating at the elevated temperature. The results of this study indicate that the hyperbranched oligomer additive may benefit lithium ion batteries to apply for mobile devices, EVs, and HEVs.

References

[1] Saeid Bashash, Scott J. Moura, Hosam K. Fathy, J. Power Sources, 196 (2011) 8747– 8754.
[2] Jonathan X. Weinert, Andrew F. Burke, Xuezhe Wei, J. Power Sources, 172 (2007) 938–945.
[3] Kandler Smith, Chao-Yang Wang, J. Power Sources, 160 (2006) 662–673.
[4] T. Kojima, T. Ishizu, T. Horiba, M. Yoshikawa, J. Power Sources, 189 (2009) 859–863.
[5] K. Zaghib, J. Dubé, A. Dallaire, K. Galoustov, A. Guerfi, M. Ramanathan, A. Benmayza, J. Prakash, A. Mauger, C.M. Julien, J. Power Sources, 219 (2012) 36-44.
[6] Humberto Joachin, Thomas D. Kaun, Karim Zaghib, Jai Prakash, J. Electrochemical Society, 156 (6) A401-A406 (2009).
[7] Arun Patil, Vaishali Patil, Dong Wook Shin, Ji-Won Choi, Dong-Soo Paik, Seok-Jin Yoon, Materials Research Bulletin 43 (2008) 1913–1942.
[8] A. Manuel Stephan, K.S. Nahm, Polymer 47 (2006) 5952-5964.
[9] N. Angulakshmi, K.S. Nahm, Jijeesh R. Nair, C. Gerbaldi, R. Bongiovanni, N. Penazzi, A. Manuel Stephan, Electrochimica Acta 90 (2013) 179-185.
[10] M. C. Smart, B. V. Ratnakumar, J. Electrochemical Society, 158 (4) A379-A389 (2011).
[11] Sheng Shui Zhang, J. Power Sources 162 (2006) 1379–1394.
[12] In Haeng Cho, Sung-Soo Kim, Soon Cheol Shin, Nam-Soon Choi, Electrochemical and Solid-State Letters, 13(11), A168-A172(2010)
[13] Fu-Ming Wanga, Shen-Chuan Lo, Chin-Shu Cheng, Jung-Hsuan Chen,

Bing-Joe Hwang, Hung-Chun Wu, Journal of Membrane Science 368 (2011)165–170.

[14] C.S. Chern, H.L. Su, J.M. Hsu, J.P. Pan, T.H. Wang, "Understanding Hyperbranched Polymerization Mechanisms", Plastics Research Online, Society of Plastics Engineers (SPE), 10.1002/spepro.003621 (2011).

[15] Fu-En Yu, Jung-Mu Hsu, Jing-Pin Pan, Tsung-Hsiung Wang, Chorng-Shyan Chern, Polym. Eng. Sci., 53, 204-211 (2013).

[16] Heng-Lei Su, Jung-Mu Hsu, Jing-Pin Pan, Tsung-Hsiung Wang, Fu-En Yu, Chorng-Shyan Chern, Polym. Eng. Sci., 51, 1188-1197 (2011).

[17] Yu-Han Li, Meng-Lun Lee, Fu-Ming Wang, Chang-Rung Yang, Peter P.J. Chu, Shueh-Lin Yau, Jing-Pin Pan, Applied Surface Science 261 (2012) 306– 311.

[18] K.-F. Chiu, H. C. Lin, K. M. Lin, C. H. Tsai, J. The Electrochemical Society, 152 (10) A2058-A2062(2005).

[19] C. C. Chen, K.-F. Chiu, K. M. Lin, H. C. Lin, C.-R. Yang, F. M. Wang, Phys. Scr. T129 (2007) 74–79.

[20] Cheng-Lun Chen, Kuo-Feng Chiu, Yan-Ru Chen, Hsin-Chih Lin, Chen Chung Chen, J. Chin. Chem. Soc. 2012, 59, 1258-1263.

[21] Sung-Chul Park, You-Min Kim, Yong-Mook Kang, Ki-Tae Kim, Paul S. Lee, Jai-Young Lee, J. Power Sources 103 (2001) 86–92.

[22] M. Risch, F. Ringleb, V. Khare, P. Chernev, I. Zaharieva, H. Dau, J. Phys. 190 (2009)12167.

[23] O.V. Komova, V.I. Simagina, O.V. Netskina, D.G. Kellerman, A.V. Ishchenko, N.A. Rudina, Catal. Today 138 (2008) 260.

[24] Doron Aurbach, J. Power Sources, 89 (2000) 206-218.

[25] Kenneth A. Walza, Christopher S. Johnson, Jamie Genthe, Lucas C. Stoiber, Walter A. Zeltner, Marc A. Anderson, Michael M. Thackeray, J. Power Sources 195 (2010) 4943–4951.